

Electronic Supplementary Information

Au nanoparticle scaffolds modulating intermolecular interactions among conjugated azobenzenes chemisorbed on curved surfaces: Tuning the kinetics of cis-trans isomerisation

Corinna Raimondo,¹ Bart Kenens,² Federica Reinders,³ Marcel Mayor,^{3,4} Hiroshi Uji-i,² and Paolo Samori^{1,}*

Contents

1. Physico-Chemical Characterization of the different sizes of nanoparticles	S-2
2. UV-Vis behavior of the systems under study by increasing the T	S-4
3. Normalization methodology employed	S-6
4. k_1 treatment - Evaluation of the kinetic constants involved during the <i>trans</i> to <i>cis</i> isomerization	S-8
5. Surface Enhanced Raman Spectroscopy (SERS)	S-9
6. Statistical characterization of the sample	S-13
7. Materials and Methods	S-14
8. References	S-15

1. Physico-chemical characterization of different sizes nanoparticles

The $^1\text{H-NMR}$ spectra of the azobenzene molecule and of the different AuNPs employed are displayed in Fig. S1. For the sake of comparison, the UV-Vis spectrum showing the different SPR of the AuNPs prior ligand-exchange reaction, i.e. when coated with a chemisorbed monolayer of alkylamine, is also displayed.

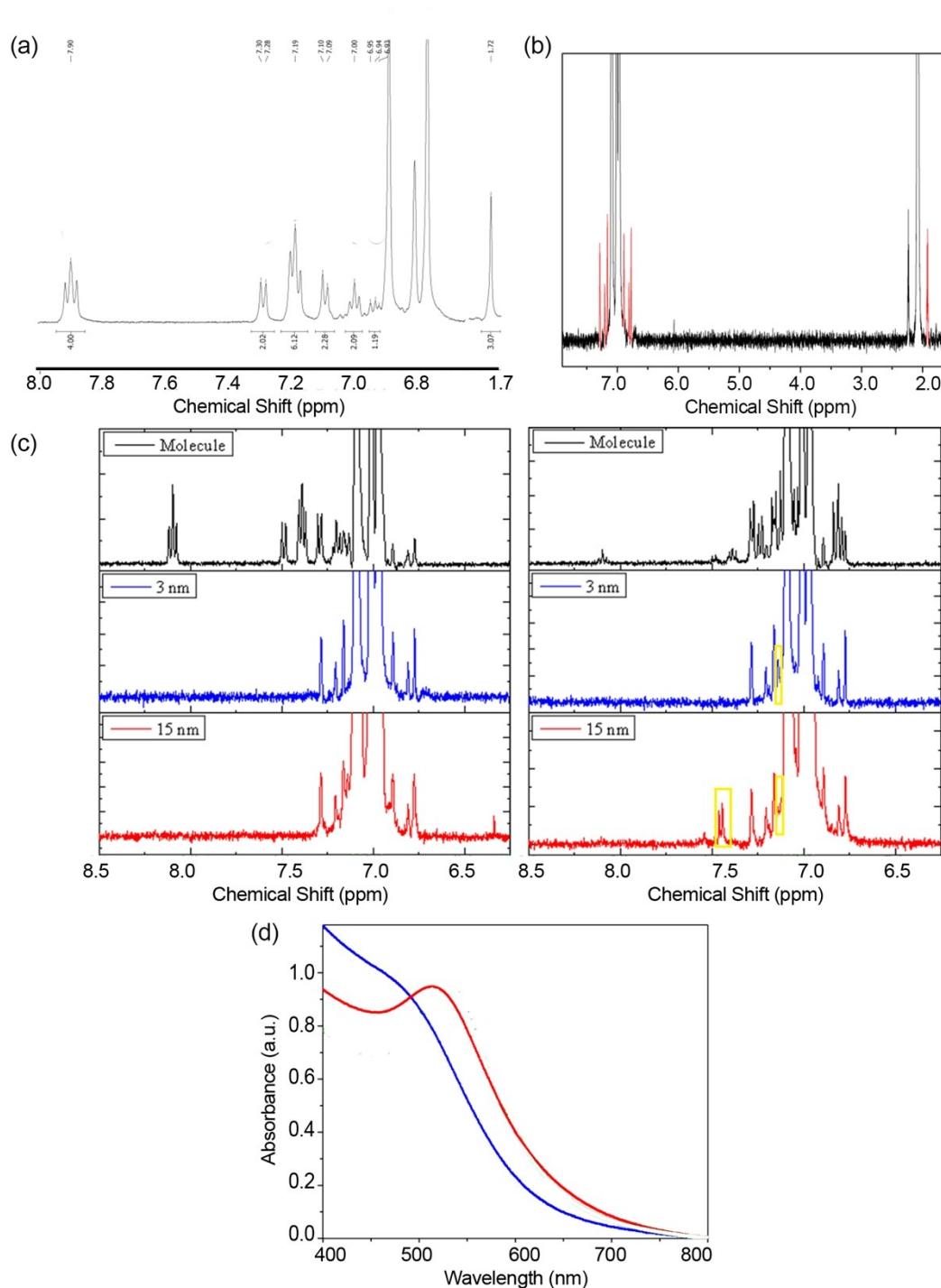


Figure S1: a) $^1\text{H-NMR}$ spectrum of the AZO molecule in toluene. b) $^1\text{H-NMR}$ spectrum of AZO on AuNP1 in toluene full range for sample purity determination (in red are highlighted the peaks that are ascribed to the azobenzene coating the

AuNPs). c) $^1\text{H-NMR}$ spectra of the aromatic region (between 8.5 and 6.25 ppm) of, from the top to bottom AZO molecule in toluene, AZO AuNP1, and AZO AuNP2. The left side shows the spectra of the *trans* form while the right one shows the ones of the *cis* form. Peaks appearing and disappearing in the different spectra are marked in yellow. d) UV-Vis characterization of the alkylamine substituted AuNPs, before ligand exchange reaction (the 3 nm and 15 nm AuNPs are plotted in blue and in red, respectively).

The possibility of performing $^1\text{H-NMR}$ on AuNPs is a very debated issue. Typical spectra reported in literature exhibit broad bands although in a few cases also more defined and sharp spectral features have been reported.¹

In order to prove that the peaks could be ascribed to a given molecule chemisorbed on the AuNPs, we acquired a series of $^1\text{H-NMR}$ spectra as synthesized, after 3 cycles of cleaning, after 20 cycles of cleanings, etc. In this way the “optimum” cleaning procedure for our system could be established: it involves 10 cycles of cleaning performed by dispersion in fresh mixture of toluene:ethanol (1:3) and subsequent centrifugation. Samples prepared using the latter procedure showed a complete absence of all the compounds utilized during synthesis.

Peaks located at different chemical shift were recorded depending on the size of the nanoparticles utilized and consistently from test to test. Given the nature of the $^1\text{H-NMR}$ spectroscopy, a different chemical shift can be ascribed to the different magnetic field experienced by the molecule studied. Being the molecule the same we propose that the reason for this behavior can be the shielding/deshielding effect of neighboring molecules, i.e. their SAM's environment.

The origin of the broad nature in the recorded $^1\text{H-NMR}$ spectra is instrumental (a 400 MHz spectrometer have been employed) and/or due to the relatively low maximum concentration of AuNPs that could be investigated because of occurrence of aggregation at higher concentrations.

The spectral difference between UV irradiated and not irradiated AuNP samples is subtle, most probably because the relevant spectral features are overlapping with the solvent peaks. On the other hand, it was not possible to use any other deuterated solvent rather than toluene because of solubility reasons. To provide greater evidence on such differences, the peaks that appear/disappear during irradiation have been marked with yellow background in Fig. S1c.

In Figure S1d the UV-Vis spectra of the two sets of nanoparticles prior substitution, when exposing a chemisorbed layer of alkylamine, are presented. Noticeably, the surface plasmon resonance absorbance gives additional prove of the nanoparticles size and narrow distribution. On the other hand, due to the aggregation/disaggregation behavior of the system the UV-Vis after substitution does not provide strong size evidence.

2. UV-Vis behavior of the systems under study by increasing the T

Being the system utilized under non-equilibrium conditions it was found that the concentration of the AuNPs in the solution played an important role when estimating the kinetic constant. Moreover, when a too high concentration was employed no disaggregation was observed; because of this reason we opted to use a concentration low enough to allow disaggregation but high enough to offer a signal as high as possible in the UV-vis spectra. The concentration was different from sample to sample, but the absorbance in “full-*trans*” state was the same. This behavior can be easily explained by keeping into consideration that the extinction coefficient of different nanoparticles sizes is different and that the UV-Vis behavior depends not only on the aggregated/disaggregated state of the nanoparticles but also on the overlapping between the single azobenzene p_z molecular orbitals that can be expected to be higher in tightly packed flat surfaces rather than in highly curved ones.

A series of spectra starting from UV-irradiated azobenzene coated AuNPs solution, i.e. *cis* isomer, and increasing step-by-step the temperature were recorded. By increasing the temperature, the *cis* isomer converts to the thermodynamically stable *trans* one. This way we can confidently start with a system fully converted to the *trans* state and with absence of π -stacking between single azobenzenes. The system measured was found being stable until 90°C. If we reach higher temperatures the AuNPs were irreversibly aggregating, most probably due to ligands desorbing from the nanoparticles as evidenced by the blue-shift in the SPR band and by naked eye. After recording the spectra (Figures S2) the concentration in the samples was adjusted in order to have 1 a.u. as absorbance. The samples were then irradiated with UV light for at least 1h to allow maximum conversion to the *cis* form; then the kinetic experiments were started.

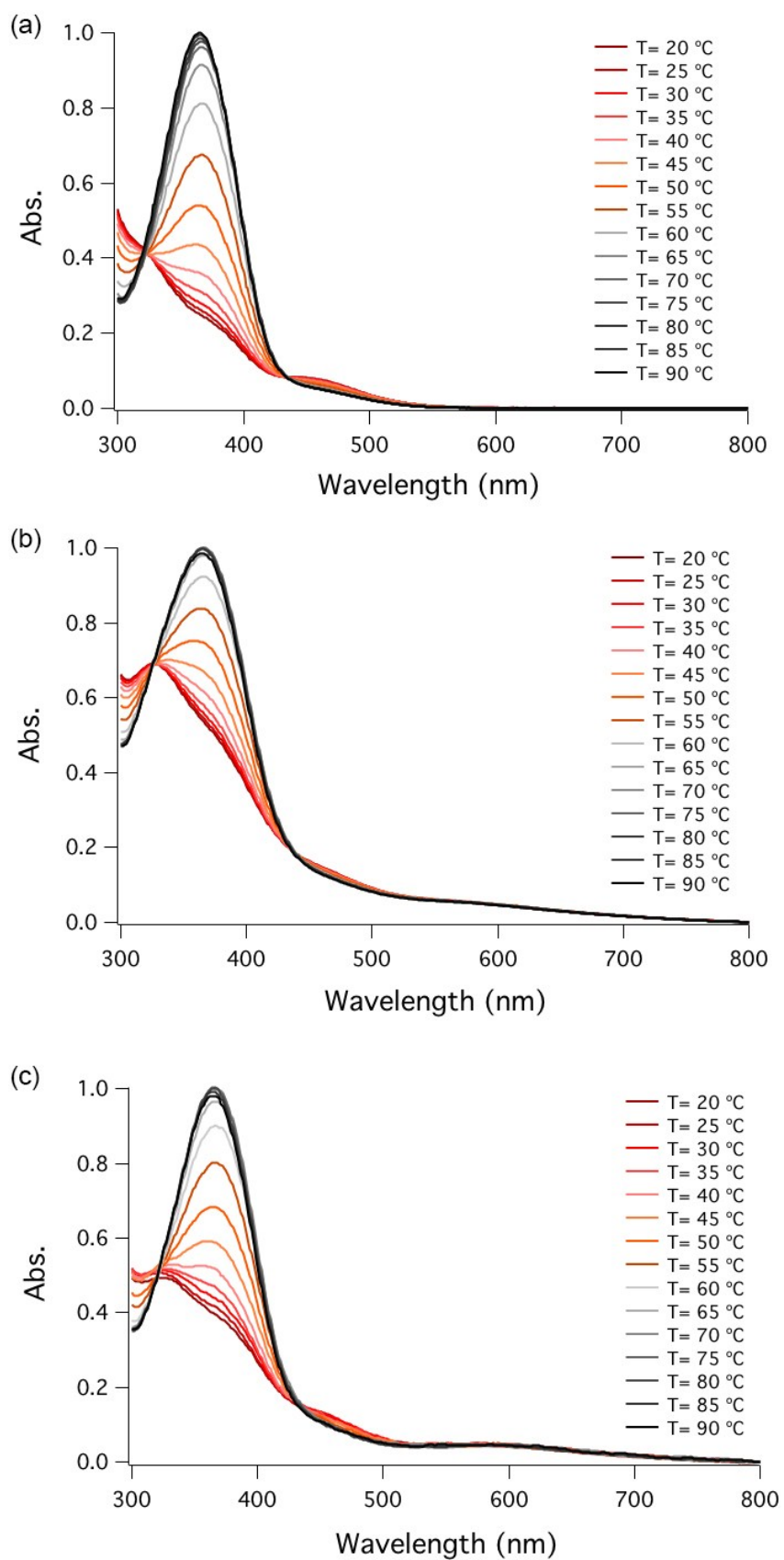


Figure S2: UV-vis spectra recorded in toluene solvent for a) neat AZO molecule, b) AZO AuNP1, c) AZO AuNP2.

3. Normalization methodology employed

A typical series of “as acquired” UV-vis absorption spectra is portrayed in Figure S3. After irradiation, the sample was left under dark and a series of spectra were recorded at discrete moments in time. During this time in the dark two are the processes involved: (i) the thermally induced back isomerization of the metastable *cis* form to the thermodynamically stable *trans* state, and (ii) the aggregation and precipitation on the AuNPs in the sample.

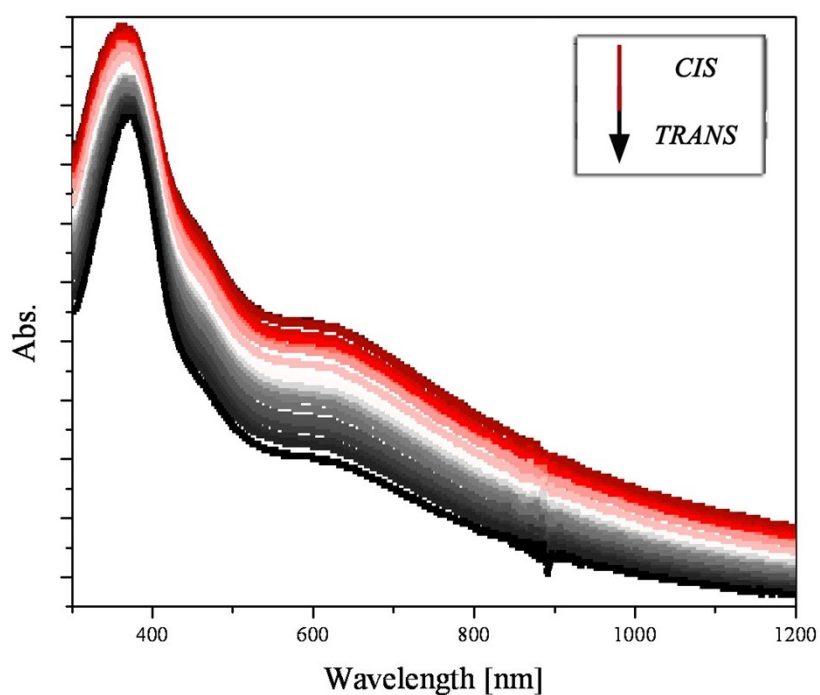


Figure S3: Series of UV-vis spectra recorded on a previously UV irradiated sample kept in the dark, i.e. allowing the azobenzene moieties to undergo isomerization from the metastable *cis* to the thermodynamically stable *trans* form.

Each single spectrum was then fitted by employing Igor Pro software into the three component of the azobenzene spectrum (Figure S4): (i) the peak at ~370 nm which is ascribed to the *trans* isomer, (ii) the peak at ~450 nm which is attributed to the *cis* isomer, and (iii) the peak between 510 and 610 nm which can be assigned the AuNP's surface plasmon resonance, its position depending on the aggregation state and the size of the AuNPs analyzed.

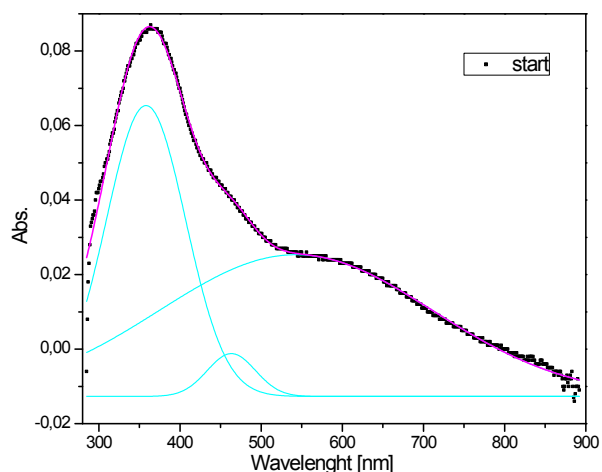


Figure S4: UV-Vis spectrum of AuNP1 recorded in toluene (in pink). In light blue are plotted the fitting of each typical peak 365 nm (*trans* azobenzene), 450 nm (*cis* azobenzene), and 600 (SPR gold nanoparticles) nm.

After fitting, a normalization for the scattering at 1200 nm first and a second one for the SPR of the nanoparticles were done in order to consider spectra based on the same number of AuNP in the optical pathway and decrease the possibility of error. An example of the resulting spectrum is displayed in Figure S5.

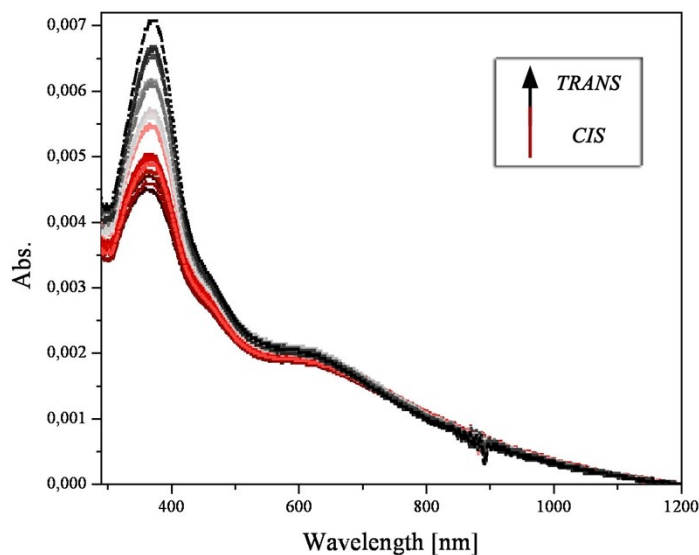


Figure S5: Typical UV-Vis spectra in toluene of an UV irradiated sample in dark after both scattering and SPR normalization.

From the absorbance at the maximum wavelength of the *trans*, which changes from sample to sample, and through the subtraction of the absorbance of the SPR at the same wavelength and via

kinetic extraction, plotting and characterization, it was possible to obtain the different logarithm of the absorbance versus time graphs (Fig. S6).

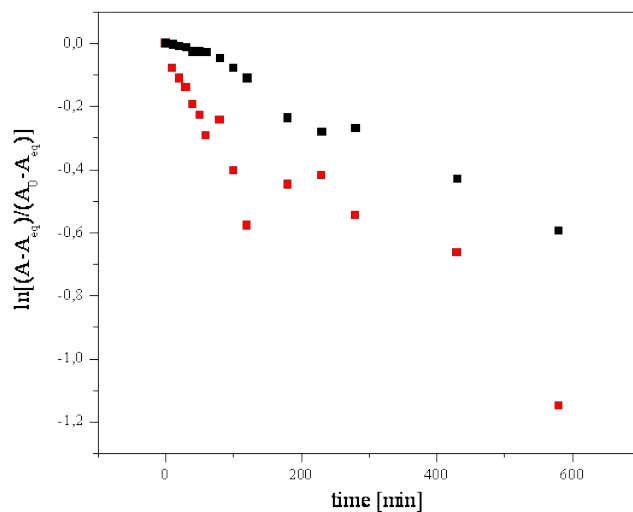


Figure S6: Logarithm of the normalized absorbance vs time of irradiates samples kept in dark, for the different systems considered. In black AZO AuNP1, and in red AZO AuNP2. Where A is the absorbance at time t, A₀ the initial one and A_{eq} at the equilibrium.

Figure 6 shows a linear behavior at short times for both nanoparticles' sizes, allowing determination of the kinetic constants early in the reaction. This determination was done by fitting the data over the first 100 minutes.

4. k_1 treatment - Evaluation of the kinetic constants involved during the *trans* to *cis* isomerization.

A kinetic analysis of the reverse *cis* to *trans* isomerization is possible, despite the high amount of variables involved. Conversely, in the case of the forward *trans* to *cis* isomerization an additional degree of complexity comes into play.

The use of UV-Vis spectroscopy does not permit to keep the sample under irradiation while measuring. Being the time needed to acquire a spectrum, at the chosen concentration, roughly 3 minutes it is not possible to compute each time the amount of reversed (*cis* to *trans*) reaction mostly from a precipitation point of view.

The data acquired did not show a linear behavior upon irradiation; hence the determination of k_1 turned out not being possible.

5. Surface Enhanced Raman Spectroscopy (SERS)

A typical SERS spectrum of the *trans* isomer of AZO when coating AuNPs is presented in Figure S7.

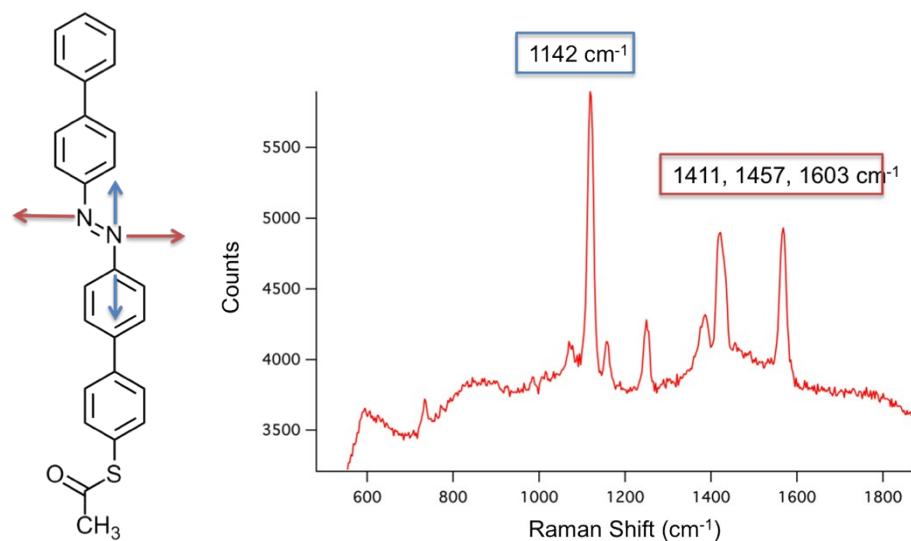


Figure S7: Right: the chemical formula of *trans* AZO (the two polarization modes are shown). Right the Raman spectrum of the *trans* AZO molecule when coating AuNP.

As reported in literature, there are two major documented changes in the SERS spectra when an azobenzene absorbed on a AuNP surface undergo *cis-trans* isomerization, i.e. a lowering of the Raman absorption resulting in a lower definition of the peaks,² and a shift of the Raman signal to give one broad absorption band³. Since the Raman spectra of the *cis* isomer acquired in solution revealed exactly the behavior reported in literature,^{2, 3}, an unique identification of the *cis* isomer is difficult. Figure S8 shows the typical *cis* isomer spectrum.

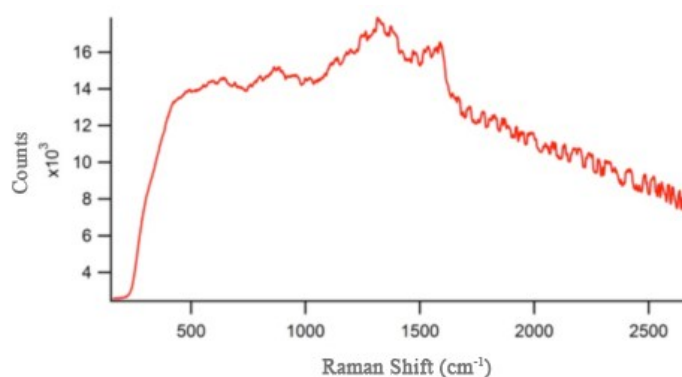


Figure S8: Typical Raman Spectrum of AZO molecule in, *cis* isomer in solution.

The same features shown for the *cis* moieties in solution (Figure S8) were observed in the case of highly aggregated nanoparticles. We ascribe this behavior to the lower intrinsic polarizability due to the high concentration of the solid sample. Figure S9 shows the typical spectra recorded when either

by moving to a more concentrated part of the sample film or by keeping the same density but UV-irradiating the sample. Since the spectral features of the *trans* isomer are well defined (see Figure S7), it was decided to evaluate the amount of *trans* in each sample and study its variation upon irradiation. Column charts in which the black part represents the amount of *trans* in the samples are presented in Figure S10.

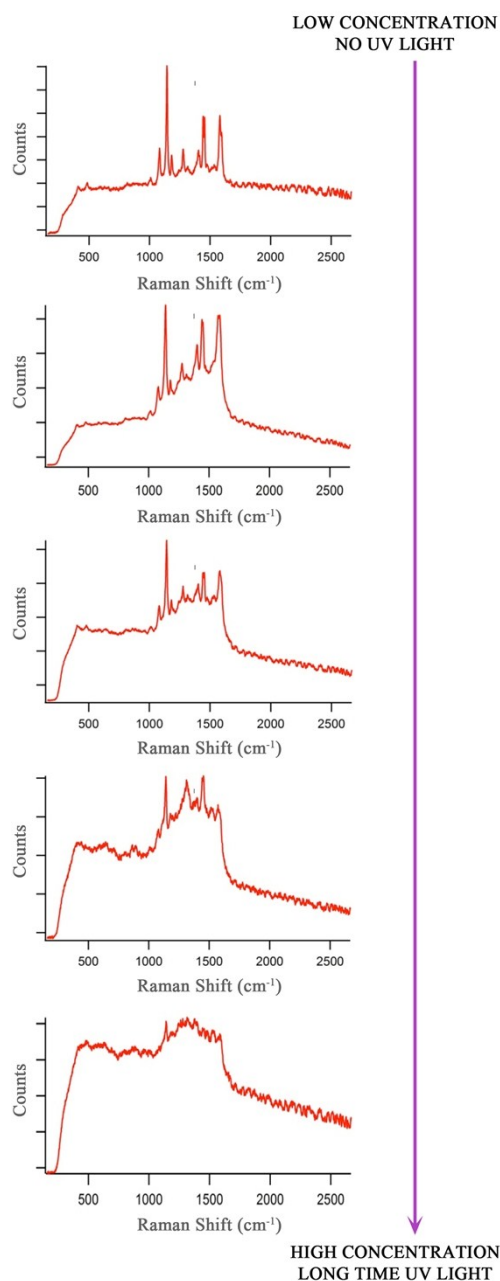


Figure S9: Dependence of the observed azobenzene spectra under prolonged irradiation or increased concentration.

The film samples of azobenzene coated AuNPs on glass coverslips were prepared by using two different procedures: the first relies on the use of nanoparticles dispersed in toluene and the latter one relies on the addition of DMF to tune the aggregation.

The substrate utilized was glass coverslips which were sonicated in acetone for 15 minutes, 2 times in sodium hydroxide for 5 minutes, and 2 times in MilliQ water for 15 minutes, then Argon blown and exposed to ozone for 15 minutes.

It was found that both increasing the concentration of nanoparticles coated with azobenzenes in the solution, thus the amount of azobenzene coated AuNP physisorbed on glass, and irradiating the thin films gave rise to similar features in the acquired SERS spectra as well as an increased intensity of the Raman spectra acquired.

Regarding the smaller nanoparticles (AZO AuNP1) we carried out a comparative study between samples deposited in *trans* or *cis* but measured after at least two days storage in dark to allow complete relaxation to the *trans* form. An average *trans* ratio equal to $78.43\% \pm 0.71$ was found. The low standard deviation between the samples prepared depositing *trans* or *cis* suggests how in a sample of small nanoparticles the variation due to deposition is not a possible source of error. Nevertheless, the ability to perform photo-triggered *cis-trans-cis* cycles of the AZO AuNP1 deposited in dark was found to be very poor; even the first irradiation did not offer appreciable results. Better results were obtained when the nanoparticles were firstly deposited in *cis* form (Figure S10).

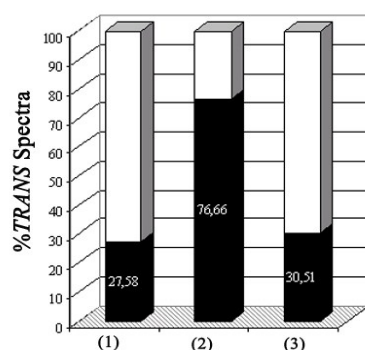


Figure S10: Percentage of *trans* azobenzene detected from left to right: (1) just after deposition under UV (sample irradiated for more than 24h), (2) after 24h time in the dark in order to allow relaxation to the *trans* form, and (3) after a further 1h of UV irradiation in situ.

As presented, the samples prepared by deposition of the *cis* isomer were able to undergo isomerization giving an appreciable difference between the percentage of *trans* moieties before and after irradiation. Unfortunately no more than three cycles were possible since the samples were then not switching anymore.

Moving to the bigger nanoparticles better results were obtained from the point of view of switching percentage. Fully *trans* spectra were recorded when depositing the sample in dark whereas no traces of *trans* isomers were detected just after deposition of the *cis*. Unfortunately no cycling was possible, likely due to fast ageing of the sample.

In general, the intensity of the Raman spectra obtained when the azobenzene is chemisorbed on 3 nm AuNPs is at least three times smaller than when absorbed on 15 nm AuNPs as shown in Figure S11. Thus further experiments focused on the bigger particles.

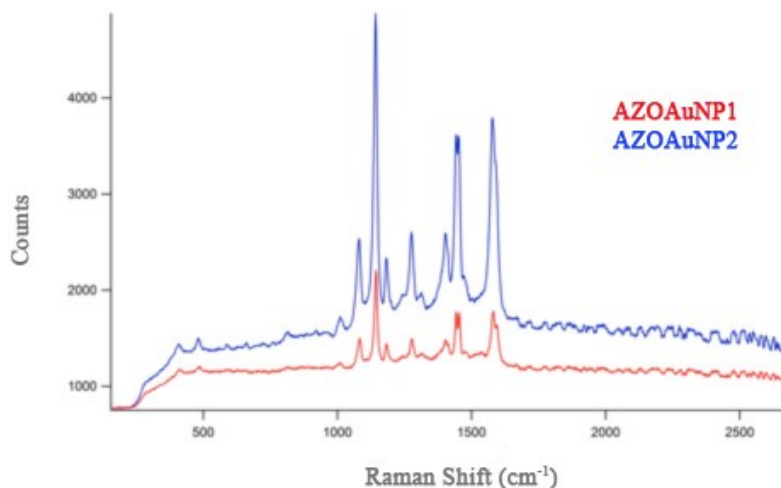


Figure S11: Typical Raman spectra of AZO *trans* isomer when absorbed on 3nm (red spectrum) or on 15nm (black spectrum) nanoparticles.

Thus, the bigger nanoparticles show higher Raman intensity. However, unfortunately the bigger the AuNPs exhibit poor *in-situ* cyclability, lowering the reliability of repeated acquisitions.

It was then decided to further investigate the smaller nanoparticles by adding a mixture of solvents, i.e. toluene: DMF (90:10), in order to tune the boiling point of the solvent and grant longer wet time to the system. 4352 spectra were acquired and averaged in order to collect a good statistics.

The best results from the point of view of switching and cyclability were obtained when drop casting in the dark 200 μ l of a solution kept at 100°C for 1-2 minutes while stirring.

The illumination/measurements sequence was consisted in the following steps:

1. Recording the first spectrum in dark
2. 2 h UV illumination
3. Recording the second Spectrum
4. 24 h in dark at room temperature
5. Recording the third Spectrum
6. 3 h UV illumination
7. Recording the fourth spectrum

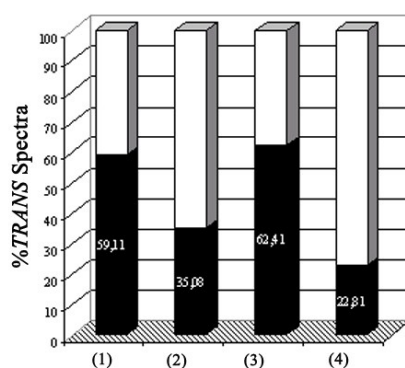


Figure S12: Comparison between the amount of *trans* AZO within irradiation: (1) 60% in the first cycle, (2) 35% in the second one, (3) 62% in the third one, (4) 23% in the fourth one.

Upon addition of DMF the investigated samples clearly retain a *cis-trans* cycle and show higher reversibility than in absence of DMF. This behavior can be ascribed to the relative high boiling point of such solvent: the samples were kept wet for longer allowing higher freedom of movement (Figure S12).

The increased intensity of the Raman spectra after UV irradiation was also found on these samples even if over the cycles a gradual decrease can be noticed as well. A possible explanation is that damage to the samples due both to the UV light used for switching and the high intensity laser used for SERS accumulates with time, thus appearing to give less *trans* signals and lower intensity.

6. Statistical characterization of the sample

A total of 34 syntheses of nanoparticles were carried out. 10 kinetic characterizations of 5 different sizes nanoparticles were done in order to better understand the systems and choose the parameters and techniques. These data were not considered in the statistic present in this paper due to the high number of parameters varied that did not allow to check if their behavior was in line with the final data shown in this paper.

NMR statistics: All the samples considered in the statistics were checked for purity via $^1\text{H-NMR}$. Six full kinetic characterizations of nanoparticles systems were done via NMR. A high relative error was measured due to relative peaks overlapping and low resolution in these samples. These samples were not considered in the statistic of this paper even if they allowed better understanding of the system itself.

SERS statistics: To get a full picture of the system, a first set of over 15750 spectra was acquired. Six different nanoparticle samples were employed: two independently synthesized samples of 3 nm azobenzene coated AuNPs, two independently synthesized samples of 15 nm AuNPs. Moreover we explored two mixed (dodecanthiol and azobenzene) coated AuNP samples, one 3 nm sized and the second one 15 nm sized. Each nanoparticle sample was deposited between 3 and 10 times to obtain statistical averaging over the deposition process and statistical representativity of the data obtained. The nanoparticles employed as well as the molecules were dispersed in toluene or in a toluene: DMF mixture in order to tune the aggregation. No full kinetic treating was done via SERS.

UV-Vis statistics: A total of 50 samples were checked both in the *trans* and in the *cis* form. 25 full kinetic characterizations were tested via UV-Vis. 9 of these 25 samples were tested in the same moment and exactly the same conditions via employment of a temperature controlled, 6 cells, stirred, spectrophotometer. Each characterization lasted 5 days.

7. Materials and Methods

All the reagents, solvents included were purchased from Aldrich. The MilliQ water was produced using a MQ water filter (Millipore- Direct Q 3).

¹H-NMR spectra were recorded on Bruker Advance 400 (400.14 MHz).

UV-Vis spectra were recorded with a Spectrophotometer UV-Vis-NIR (Shimadzu UV-3600) whereas for simultaneous measurements of more samples and temperature control a JASCO V-670 equipped with a PAC-743R sample holder (6 cells and temperature control) was employed.

Raman spectroscopy and Raman mapping were performed employing a CombiScope (AIST-NT) on an invert optical microscope (Nikon TiU) equipped with a 100x oil immersion objective (Nikon Plan Fluor 100x N.A. = 1.3). Two spectrometers were employed: an Andor, Shamrock 303 or Horiba, iHR320 both coupled with an Electron magnifying CCD camera (Andor, Newton DU970P-BV or DU920P-BR-DD, respectively). The excitation source was a He-Ne laser (JDS Uniphase, 1145P, 28 mW or Research Electro-Optics, Inc., 32413, 35.0mW, 632.8 nm wavelength). An interference filter (Chroma technology corporation, Z633/x10) was employed in order to selectively choose the 632.8 nm radiation from the He-Ne lasers. The samples excitation was performed by mean of a circular polarized light, compensating the polarization shifts induced by the dichroic mirrors through $\lambda/4$ and $\lambda/2$ wave-plates. After passing through the dichroic mirror (Z633RDC, Chroma Technology Co.) equipped with an additional spectral filter (HQ645LP, Chroma Technology Co.) the Raman scattering was collected utilizing the CCD camera.

The irradiation lamp was a UV lamp with λ_{\max} of emission centered around 366 nm (Benda NU-8 KL).

The TEM images were acquired by employing a Philips CM100 transmission electron microscope at 80kV equipped with a 2000 by 2000 pixel charge-coupled Veleta camera from Olympus. The particles were deposited by drop-casting the colloidal dispersion on a carbon coated gold-plated copper grid and air-dried.

8. References.

1. a) M. J. Hostetler, J. E. Wingate, C. J. Zhong, J. E. Harris, R. W. Vachet, M. R. Clark, J. D. Londono, S. J. Green, J. J. Stokes, G. D. Wignall, G. L. Glish, M. D. Porter, N. D. Evans and R. W. Murray, *Langmuir*, 1998, **14**, 17-30; b) G. C. Lica, B. S. Zelakiewicz and Y. Y. Tong, *J Electroanal Chem*, 2003, **554**, 127-132; c) Y. Song, A. S. Harper and R. W. Murray, *Langmuir*, 2005, **21**, 5492-5500; d) A. C. Templeton, S. W. Chen, S. M. Gross and R. W. Murray, *Langmuir*, 1999, **15**, 66-76.
2. Y. B. Zheng, J. L. Payton, C. H. Chung, R. Liu, S. Cheunkar, B. K. Pathem, Y. Yang, L. Jensen and P. S. Weiss, *Nano Lett*, 2011, **11**, 3447-3452.
3. U. Jung, M. Muller, N. Fujimoto, K. Ikeda, K. Uosaki, U. Cornelissen, F. Tuzcek, C. Bornholdt, D. Zargarani, R. Herges and O. Magnussen, *J Colloid Interf Sci*, 2010, **341**, 366-375.